

ОБЪЕДИНЕННЫЙ
ИНСТИТУТ
ЯДЕРНЫХ
ИССЛЕДОВАНИЙ

Дубна

96-429

E4-96-429

V.B.Belyaev, O.I.Kartavtsev, V.I.Kochkin, E.A.Kolganova

DECAY RATES AND γ -RAY SPECTRA
OF HeH μ SYSTEMS

Submitted to «Zeitschrift für Physik D»

1996

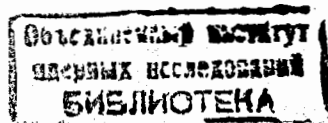
1 Introduction

During last decades, study of charge-nonsymmetric muonic molecules attracts a continuous interest both theoretically and experimentally. The first measurements of the yield of γ -rays due to the decay of the $\text{He}\mu$ molecules [1, 2] revive interest in the investigation of this system. In the recent experiments [3] γ -rays spectra of ${}^3,4\text{He}\mu$ systems have been measured with very high resolution. Besides, the first measurement of γ -rays spectra from the ${}^3,4\text{He}\mu$ - molecules has been done [4]. These results call for theoretical treatment of comparable accuracy. One should emphasize that these experiments provide direct observation of a mesic molecule. In opposite to $\text{HeH}\mu$, other mesic molecules can be observed only in indirect experiments.

All the above mentioned experiments give evidence of the significant role of the nonradiative decay channel. Strong isotopic dependence of this process was found both experimentally and in the different calculations [5]-[8].

The production of charge-nonsymmetric muonic molecules plays an important role in the kinetics of muons in media. The reason is the comparatively low probability of the direct muon transfer from the ground-state muonic hydrogen atom to the helium nucleus. Therefore, the muon transfer proceeds via the formation of the molecule in the intermediate state [9].

The important decay channel of $\text{HeH}\mu$ systems is the nuclear transition. The investigation of a nuclear reaction at typical mesomolecular energies has a fundamental importance due to absence of any experimental data on the strong interaction of charged particles in this energy range. This information is also significant in astrophysical problems. ${}^3\text{He}$ interaction is of special interest due to the existence of near-threshold resonance ${}^5\text{Li}(\frac{3}{2}^+)$ (mirror to the well known ${}^5\text{He}(\frac{3}{2}^+)$ resonance). Generally, the near threshold resonances in the interaction of light nuclei:



$t + ^3\text{He}$, $d + ^6\text{Li}$, $d + ^7\text{Li}$ can lead to enhancement of nuclear transition rate in muonic molecules [10]. One should mention the absence of electron screening in the investigation of the low-energy light nuclei interaction in muonic hydrides. The treatment of the screening effects in the experiments with colliding nuclei is an essential problem [11] and special efforts are needed for the reliable consideration.

Qualitatively properties of the $\text{HeH}\mu$ system can be described as follows. The repulsion in the $\text{He}\mu + \text{H}$ channel hinders the binding of the systems under consideration and only a 3-body resonant state can be formed. States like that are supported by the attractive polarization potential in the $\text{H}\mu + \text{He}$ channel and, therefore, are clustered.

The goal of this paper is the unified treatment of different properties of the $^3, ^4\text{He}^{1,2}\text{H}\mu$ systems, namely, radiative and non-radiative decay rates and eigenenergies for all possible values of the total angular momentum. The competition of two decay channels and the strong isotopic dependence of the nonradiative decay rates are of special interest. A comparison of the calculated γ -rays spectra with recent experiments allows the determination of the total angular momentum of $\text{HeH}\mu$ molecules. Besides, the investigation of the nonradiative decay rate provides information on the behavior of the wave function at small distances, which is important for description of nuclear transitions.

As in the previous paper [12], the approach based on the hyperspherical "surface" functions method [13], has been applied in this paper. A number of three-body systems, such as $e^+e^-e^-$, $e^+\text{H}$, H^- , $d\text{t}\mu$ were successfully described in the framework of this method [14]-[18]. This method allows the reliable treatment of the posed problems due to the following reasons. The method operates with a discrete set of coupled one-dimensional differential equations. Physical boundary conditions for their solution can easily be formulated. Moreover, coupling of channels turns out

to be rather small in the calculation of charge-nonsymmetrical mesic molecules and allows one to use the decoupled one-level approximation.

The article is organized in the following way. The description of the method will be given in the next section, section 3 contains numerical results, section 4 - outlook and discussion.

2 Method

2.1 Hyperspherical surface functions approach

The hyperspherical surface function (HSF) approach is well known in literature [13]-[18] and there is no need to describe it in detail. The approach used is mainly the same as in the preceding paper [12]. For this reason the notation and units of this paper will be used below. The three-body wave function for the state of the total angular momentum L and its projection M can be expanded over the Wigner D-functions

$$\Psi^{LM}(\vec{x}, \vec{y}) = \sum_K D_{MK}^L(\beta, \gamma, \delta) \Phi_K^L(x, y, \theta), \quad (1)$$

where two of the Euler angles determine a direction of the inter-nuclear vector \vec{x} .

Taking into account in (1) only the term with $K = 0$ one can obtain the ansatz

$$\Psi^{LM}(\vec{x}, \vec{y}) = Y_{LM}(\hat{x}) \Phi^L(x, y, \theta), \quad (2)$$

Expression (2) means that the total angular momentum L is carried mainly by heavy particles. For $L = 0$ the ansatz (2) is exact and for $L \neq 0$ this approximation should be reliable due to the smallness of mass ratios of muon and nuclei. Indices L and M will be omitted below to simplify the notation.

In the framework of the HSF method the following expansion of Φ will be used

$$\Phi(\rho, \Omega) = \rho^{-5/2} \sum_n u_n(\rho) \varphi_n(\Omega; \rho), \quad (3)$$

The HSF $\varphi_n(\Omega, \rho)$ are finite solutions of the eigenvalue problem

$$[\Delta_\Omega - \frac{\rho^2}{4} \sum_{s=1}^3 \frac{q_s}{x_s} + \lambda_n(\rho)] \varphi_n(\Omega; \rho) = 0. \quad (4)$$

Note that the functions $\varepsilon_n(\rho) = \lambda_n(\rho)/\rho^2$ play a role of the effective potentials. The channel functions $u_n(\rho)$ satisfy the system of one-dimensional equations [12]. In this approach, the coupling terms

$$\begin{aligned} Q_{ni}(\rho) &= \langle \varphi_n | \frac{\partial}{\partial \rho} \varphi_i \rangle, \\ P_{ni}(\rho) &= \langle \frac{\partial}{\partial \rho} \varphi_n | \frac{\partial}{\partial \rho} \varphi_i \rangle, \end{aligned} \quad (5)$$

are responsible for the nonradiative transitions. Since the direct computation of $Q_{ni}(\rho)$ and $P_{ni}(\rho)$ is rather difficult, the following exact expressions have been used:

$$\begin{aligned} Q_{ni}(\rho) &= -\frac{\rho}{4} (\lambda_i - \lambda_n)^{-1} \langle \varphi_n | \sum_{s=1}^3 \frac{q_s}{x_s} | \varphi_i \rangle, \\ P_{ni}(\rho) &= -(Q_{ni}^2). \end{aligned} \quad (6)$$

The form (6) allows one to avoid the calculation of the derivatives of the "surface" functions on the parameter ρ .

The variational approach has been applied to solve equation (4). The "surface" functions have been chosen as a linear combination of trial functions from the following set:

$$\phi_{nl}^{(\sigma)}(\alpha_\sigma) P_l(\cos \theta_\sigma), \quad \sigma = 2, 3 \quad (7)$$

$$\sin^l \alpha_3 C_{n-l-1}^{l+1}(\cos \alpha_3) P_l(\cos \theta_3), \quad n > 0, \quad n > l \geq 0, \quad (8)$$

where

$$\phi_{nl}^{(\sigma)}(\alpha) = R_{nl} \left(\frac{|q_\sigma|}{n} \rho \cos \frac{\alpha}{2} \right), \quad (9)$$

$$R_{nl}(t) = \exp(-t/2) t^l L_{n-l-1}^{2l+1}(t)$$

In equations (7) - (9) $P_l(x)$, $L_m^k(x)$, $C_n^m(x)$ are the Legendre, Laguerre and Gegenbauer polynomials. The set of trial functions has been chosen in the form (7) in order to describe properly the three-body wave-function at both large and small interparticle distances. Expression (7) describes the system separated into two clusters. In this case, one of the clusters is a hydrogen-like atom and hydrogen-like functions (9) will be proper trial functions for a large hyperradius. While $\sigma = 2$ and 3, expression (7) is the wave function of the $\text{He}\mu$ and $\text{H}\mu$ - mesic atoms, respectively. Expression (8) describes the configuration with all three particles close to each other. In this case the kinetic energy term Δ_Ω dominates in (4) and eigenfunctions (8) of the operator

$$\square = \frac{1}{\sin^2 \alpha} \left[\frac{\partial}{\partial \alpha} (\sin^2 \alpha \frac{\partial}{\partial \alpha}) + \frac{1}{\sin \theta} \frac{\partial}{\partial \theta} (\sin \theta \frac{\partial}{\partial \theta}) \right] \quad (10)$$

are used. The set of trial functions (7) - (9) can easily be adjusted to the different values of the parameter ρ . For this purpose numbers of channel-type functions (7) and hyperspherical harmonics (8) have been changed with changing ρ . It is necessary to emphasize that the dependence of the numbers of the trial functions on the parameter ρ has not been exploited in analogous calculations. This dependence gives rise to more flexibility of the basis and allows one to avoid numerical instabilities when solving equation (4).

As a result of the solution of equation (4), eigenpotentials $\varepsilon_n(\rho)$ and coupling terms $Q_{12}(\rho)$, $P_{12}(\rho)$ have been obtained. Next, hyperradial equations have been solved and the physical characteristics have been calculated.

2.2 He H μ - resonant state

The following properties of the systems under consideration should be taken into account in the calculation of the resonance energy and wave function. The dominant cluster structure of the

type $\text{He} + \text{H}\mu$ is a reason to use in this calculation the second effective potential $\varepsilon_2(\rho)$. As it has already been mentioned, this potential has an attractive part and supports the resonant state.

Next, the widths of such resonances are rather narrow. Therefore, coupling with the open channel described by the eigenpotential $\varepsilon_1(\rho)$ can be neglected. Indeed, the calculated coupling terms $Q_{12}(\rho)$ and $P_{12}(\rho)$, as it is clear from Fig. 1, are small in the region, where the component u_2 of the resonant wave function is localized. This consideration brings to the well-known "uncoupled adiabatic approximation" for the calculation of energy E_R and the radial wave function $u_2(\rho)$ as an eigenvalue problem:

$$\begin{cases} \left[\frac{d^2}{d\rho^2} - \frac{15}{4\rho^2} - \varepsilon_2(\rho) - P_{22}(\rho) + E_R \right] u_2(\rho) = 0 \\ u_2(0) = u_2(\infty) = 0. \end{cases} \quad (11)$$

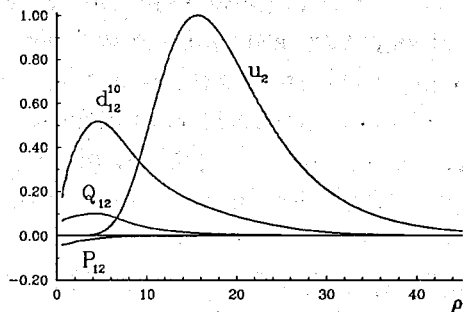


Figure 1: Coupling terms $Q_{12}(\rho)$, $P_{12}(\rho)$, the dipole moment distribution $d_{12}^{10}(\rho)$ and the hyperradial wave function $u_2(\rho)$ for the system ${}^3\text{HeH}\mu$. Units are described in the text; u_2 is presented in an arbitrary scale.

2.3 Nonradiative decay rate

Possible final states in the decay of $\text{HeH}\mu$ are the scattering ones of hydrogen nucleus on the $\text{He}\mu$ atom. Eigenpotential $\varepsilon_1(\rho)$ as-

ymptotically approaches the $\text{He}\mu$ atom ground state energy $\varepsilon_{1\infty}$ and describes the dynamics in the open channel.

Following the arguments of section 2.2, the scattering wave function $u_1(\rho)$ can be found as a solution of the boundary problem at fixed $\text{HeH}\mu$ resonance energy $E = E_R$:

$$\begin{cases} \left[\frac{d^2}{d\rho^2} - \frac{15}{4\rho^2} - \varepsilon_1(\rho) - P_{22}(\rho) + E \right] u_{1k}(\rho) = 0, \\ u_{1k}(0) = 0, \\ u_{1k}(\rho) \xrightarrow{\rho \rightarrow \infty} \sin(k\rho + \delta), \end{cases} \quad (12)$$

where $k = (E - \varepsilon_{1\infty})^{1/2}$.

One should mention that transition to the channels with the $\text{He}\mu$ atom in the excited states will be suppressed due to exponentially small overlapping of the initial and final state wavefunctions.

Due to the smallness of coupling the interchannel transition can be defined by the matrix element M of the coupling operator:

$$M_k = \int_0^\infty d\rho u_{1k}(\rho) \left[Q_{12}(\rho) \frac{d}{d\rho} + \frac{d}{d\rho} Q_{12}(\rho) - P_{12}(\rho) \right] u_2(\rho). \quad (13)$$

The radiationless decay rate λ has the form:

$$\lambda = \frac{1}{k} |M_k|^2. \quad (14)$$

2.4 Spectra and total rates of the radiative decay

The main contribution to the radiative decay comes from the dipole transitions. γ -ray spectra and total rates of all dipole transitions from the states with angular momenta $L = 0, 1$ have been calculated. The final state radial wave function $u_{1k}(\rho)$ describing relative motion of a hydrogen isotope nucleus and $\text{He}\mu$ -atom is a solution of equation (12) at the energy carried by these particles $E = E_R - E_\gamma$.

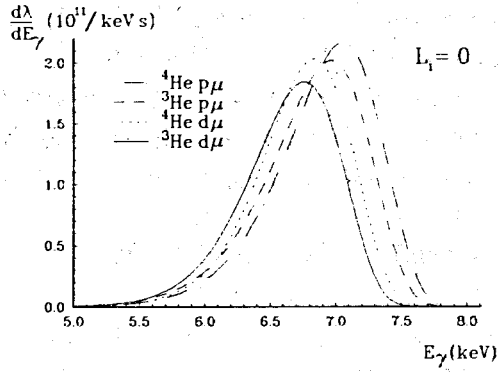


Figure 2: γ -ray spectra of the $^{3,4}\text{HeH}\mu$ system in the initial states with the total angular momentum $L_i = 0$.

The dipole transition rate per unit energy (spectrum of γ -rays) is given by

$$\frac{d\lambda_\gamma}{dE_\gamma} = \frac{1}{3} \frac{(\alpha E_\gamma)^3}{\pi k} \cdot \frac{1}{2L_i + 1} \sum_{L_f} |\langle \Psi_f || \mathbf{d} || \Psi_i \rangle|^2, \quad (15)$$

where α is the fine structure constant, $k^2 = E_R - \varepsilon_{1\infty} - E_\gamma$ and L_i, L_f are total angular momenta of the initial and final states, respectively. Dipole operator \mathbf{d} is expressed in terms of the scaled Jacobi coordinates \mathbf{x}, \mathbf{y}

$$\mathbf{d} = \mathbf{y} \frac{-(m_2 + m_3) - 3m_1}{(m_1 + m_2 + m_3)\sqrt{m_2 + m_3}} + \mathbf{x} \frac{2m_2 - m_3}{\sqrt{m_2 m_3 (m_2 + m_3)}}. \quad (16)$$

The representations (2) and (3) for the initial and final state wave functions Ψ_i, Ψ_f reveal the following form of the reduced matrix element in (15)

$$\langle \Psi_f || \mathbf{d} || \Psi_i \rangle = \int_0^\infty d\rho u_{1k}(\rho) d_{L_f L_i}(\rho) u_2(\rho). \quad (17)$$

The distribution of the dipole moment $d_{L_f L_i}(\rho)$ is an integral over angular variables of the dipole operator and HSF of the final state

$\varphi_1(\Omega, \rho)$ and initial state $\varphi_2(\Omega, \rho)$. The typical behavior of the dipole moment distribution can be seen in Fig. 1, where $d_{10}(\rho)$ for the system $^3\text{HeH}\mu$ is plotted.

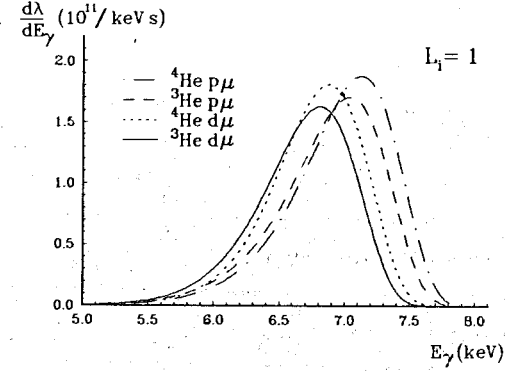


Figure 3: γ -ray spectra of the $^{3,4}\text{HeH}\mu$ system in the initial states with the total angular momenta $L_i = 1$.

3 Results of calculation

The theory described in the preceding sections have been used to calculate the binding energies $E_B = \varepsilon_{2\infty} - E_R$, γ -ray spectra of radiative decay $\frac{d\lambda}{dE_\gamma}$, radiative decay rates $\lambda_\gamma = \int \frac{d\lambda}{dE} dE$ and nonradiative decay rates λ .

The systems $^4\text{HeH}\mu, ^4\text{HeH}\mu, ^3\text{HeH}\mu, ^3\text{HeH}\mu$ in the states with the total angular momenta $L = 0, 1, 2$ have been considered.

Calculated values and available results of other authors are presented in Table 1. The type and number of trial functions, interval of radial integration, masses of particles and resulting accuracy of the numerical procedure are the same as in [12].

To demonstrate the isotopic dependence all theoretical γ -ray spectra for the decay from $L_i = 0, 1$ states are presented on Fig. 2 and 3.

Table 1: Calculated binding energies $E_B(eV)$ and decay rates λ, λ_γ ($10^{11} s^{-1}$) of the systems ${}^3, {}^4\text{He}^{12}\text{H}\mu$, * - present results.

system	ref.	L=0			L=1			L=2	
		E_B	λ	λ_γ	E_B	λ	λ_γ	E_B	λ
${}^4\text{He}d\mu$	[5]				58.22	1.67			
	[8]				58.225303	1.80			
	[19]				57.84		1.69		
	[6]	77.96	2.3		56.10	2.4			
	[7]	78.7	1.85	1.94	57.6	1.38	1.74	20.3	0.9
	*	77.49	0.73	1.76	55.74	1.20	1.58	17.49	1.04
${}^3\text{He}d\mu$	[5]				48.42	5.06			
	[8]				48.420890	5.29			
	[19]	70.74		1.75	47.90		1.55		
	[6]	69.96	8.0		46.75	7.0			
	[7]	70.6	3.58	1.80	48.2	2.77	1.58	9.6	1.54
	*	69.37	2.87	1.64	46.31	3.22	1.44	7.11	1.74
${}^4\text{He}p\mu$	[19]				50.0		1.92		
	[6]	74.36	71		41.17	38			
	[7]	75.4	35.4	2.24	45.4	24.8	1.89		
	*	80.64	70.7	2.02	47.45	38.5	1.74		
${}^3\text{He}p\mu$	[6]	67.70	100		33.85	46			
	[7]	69.0	47.3	2.11	38.1	31.6	1.74		
	*	72.76	97.7	1.91	38.82	46.7	1.60		

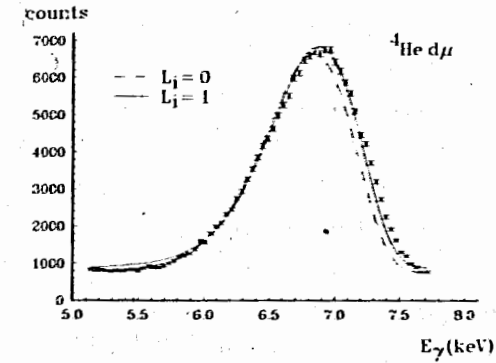


Figure 4: Comparison of the normalized theoretical γ -ray spectra with the experiment for the ${}^4\text{He}d\mu$ system.

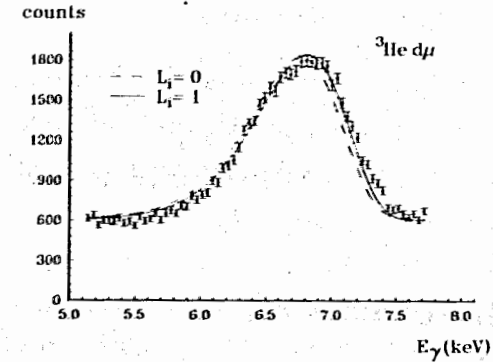


Figure 5: Comparison of the normalized theoretical γ -ray spectra with the experiment for the ${}^3\text{He}d\mu$ system.

At the moment new and accurate γ -ray spectra from the decay of the ${}^4\text{He}d\mu$, ${}^3\text{He}d\mu$ and ${}^4\text{He}p\mu$ systems are measured in the experiments [3] and [4]. Since the absolute yield of γ -ray was not obtained in the experiments and due to the presence of a background, only shapes of the experimental and theoretical spectra can be compared. Taking these facts into account, one can assume that the following two-parameter normalization procedure should be applied to fit the experimental spectrum

$$\left(\frac{d\lambda}{dE}\right)_n = A + B \left(\frac{d\lambda}{dE}\right)_{th}$$

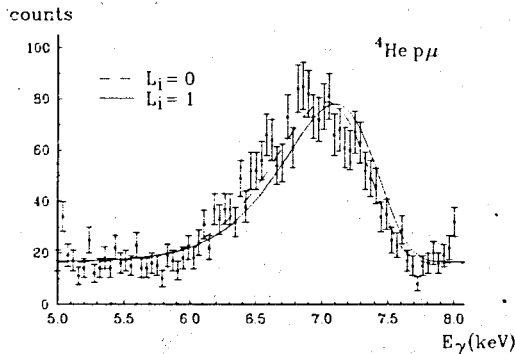


Figure 6: Comparison of the normalized theoretical γ -ray spectra with the experiment for the ${}^4\text{He} p \mu$ system.

where the parameters A and B are determined through the least squares procedure. The normalized theoretical spectra $\left(\frac{d\lambda}{dE}\right)_n$ for $L_i = 0, 1$ are presented in comparison with the experiment in Figs. 4 – 6.

4 Outlook and discussion

The lifetime of the ${}^3,4\text{He} {}^1,2\text{H} \mu$ systems is determined by a competition of two main decay channels: radiative and nonradiative ones. It is important that both rates are comparatively small and sensitive to the fine details of the wave function. In this respect, the strong isotopic dependence of the nonradiative decay rate is of special interest for studying the small components of the wave function.

All the calculations (see Table 1) support the strong isotopic dependence of the nonradiative decay rate noted in experiments [1]–[4]. This rate decreases rapidly with increasing reduced mass of two heavy particles. Qualitatively, the muon transfer in the nonradiative decay process takes place mainly at small internuclear distances. Due to the cluster $\text{He} + \text{H} \mu$ structure, two

heavy particles should penetrate under the potential barrier to bring together. As a consequence, the transition probability decreases exponentially with increasing reduced mass. Besides, the nonradiative decay rate is sensitive to the total angular momentum and reduced mass due to the interference of the initial and rapidly oscillating final state wave functions.

Opposite to the nonradiative decay channel, the radiative decay rate (as it is clear from Table 1) depends slightly on isotope masses. The different isotopic dependence can be explained by the different spatial structure of the transition operators. Really, the main contribution to the matrix element of the radiative transition originates from the region of comparatively large $\rho \sim 10 - 15$, where the initial state wave function is not sensitive to the nucleus masses. Considering the position of γ -ray spectra presented in Fig. 2 and 3, one can conclude that the total radiative decay rate increases with the γ -ray energy both for $L_i = 0$ and $L_i = 1$. A change of the spectrum position for different isotopes is a consequence of a change of the threshold energies for the initial and final states. As a matter of fact, the transition energy increases slightly with increasing mass of the helium isotopes due to lowering of the first eigenpotential. At the same time, increasing the mass of the hydrogen isotope gives rise to a bit more decreasing in the transition energy due to the lowering of the second eigenpotential.

Despite the slow isotopic dependence of the radiative decay, the branching ratio for this channel $\kappa = \lambda_\gamma / (\lambda_\gamma + \lambda)$ reveals the significant isotopic effect due to the strong isotopic dependence of the radiationless decay rate. Since the yield of radiation is mainly defined by the branching ratio κ , the isotopic effect appears as a significant difference in the intensities of the experimental radiative spectra Figs. 4 – 6. Besides, the ratio of κ for the ${}^3\text{He} d \mu$ and ${}^4\text{He} d \mu$ systems $\xi = \frac{\kappa({}^3\text{He} d \mu)}{\kappa({}^4\text{He} d \mu)} = 0.46$ was obtained in the exper-

iment [3]. Present values are close enough to the experimental one both for the states with $L_i = 1$ ($\xi = 0.53$) and for the states with $L_i = 0$ ($\xi = 0.51$).

The shapes of γ -ray spectra for different total angular momenta $L_i = 0, 1$ are very similar and the $L_i = 1$ spectra are slightly shifted to higher energies in comparison with the $L_i = 0$ ones. However, the accuracy of recently measured γ -ray spectra of ${}^3, {}^4\text{Hed}\mu$ [3] is high enough to distinguish the $L_i = 0, 1$ theoretical spectra on qualitative level. For this reason, the experimental and theoretical γ -ray spectra of these systems for the total angular momenta $L_i = 0, 1$ have been compared in Fig. 4 and 5. From the comparison, one has to conclude that radiative transitions take place from the $L_i = 1$ state of the ${}^3\text{Hed}\mu$ and ${}^4\text{Hed}\mu$ molecules. One should mention that this result is the first definite assignment of the total angular momentum of the ${}^3, {}^4\text{Hed}\mu$ - molecules observed in experiment.

The definite conclusion about the total angular momentum of the ${}^3, {}^4\text{Hed}\mu$ molecules can not be made due to the low γ -ray yields and, therefore, the low relative experimental accuracy. The reason is the low branching ratio κ for these molecules, i.e., the nonradiative decay dominates over the radiative one.

In conclusion one should list a number of problems with concerns of the $\text{HeH}\mu$ systems still waiting for more refined investigations. Bearing in mind the last measurements, the reliable treatment of the formation probability is needed. While the probability of the muon transfer via the intermediate formation of muonic molecules exceeds the probability of the direct one, the last process cannot be fully neglected for some isotopes. The accurate calculation of the direct transfer is desirable to clear up its contribution.

As it has already been mentioned, calculation of the nuclear transition rates is of special importance. Probability of nuclear transitions are much higher from the states with $L = 0$ than

from the $L_i = 1$ ones. In this respect, the rates of intermolecular conversion $L_i = 1 \rightarrow L = 0$ are essential. These rates recently calculated in [20] are comparable with the decay rates into main channels. It seems that this result is not in agreement with the conclusion of this paper on the preferable decay mode from the $L_i = 1$ state.

Acknowledgement. Authors are grateful to B. Gartner and S. Tresch for providing us with the experimental data and to L. Schellenberg and T. Mamedov for useful discussion. One of the authors (V.B.B.) would like to thank Physikalishes Institute of Bonn University for hospitality.

References

- [1] T. Matsuzaki, K. Ishida, K. Nagamine, Y. Hirata and R. Kadono, *Muon Cat. Fusion* **2**, 217 (1988)
- [2] K. Ishida, S. Sakamoto, Y. Watanabe, T. Matsuzaki and K. Nagamine, *Hyperfine Interactions* **82**, 111 (1993)
- [3] B. Gartner et al., *Proc. of Int. Symp. on Muon Cat. Fusion. Dubna, 1995, Hyperfine Interactions*, in press.
- [4] S. Tresch et al., *Proc. of Int. Symp. on Muon Cat. Fusion. Dubna, 1995, Hyperfine Interactions*, in press.
- [5] Y. Kino and M. Kamimura, *Hyperfine Interactions* **82**, 195 (1993)
- [6] S.S. Gershtein and V.V. Gusev, *Hyperfine Interactions* **82**, 185 (1993)
- [7] A.V. Kravtsov, A.I. Mikhailov and V.I. Savichev, *Hyperfine Interactions* **82**, 205 (1993)
- [8] V.I. Korobov, *Proc. of Int. Symp. on Muon Cat. Fusion. Dubna, 1995, Hyperfine Interactions*, in press.

- [9] A.V. Kravtsov et al., Phys. Lett. A83, 379 (1981)
- [10] S.A. Rakitynsky, S.A. Sofianos, V.B. Belyaev and V.I. Korobov, Phys. Rev. A54, 1242 (1996)
- [11] T.D. Shoppa, S.E. Koonin, K. Langanke and R. Seki, Phys. Rev. C48, 837 (1993)
- [12] V.B. Belyaev, O.I. Kartavtsev, V.I. Kochkin and E.A. Kolganova, Phys. Rev. A52, 1765 (1995).
- [13] J.H. Macek, J. Phys. B1, 831 (1968)
- [14] M. Fabre de la Ripelle, M.I. Haftel and S.Y. Larsen, Phys. Rev. A44, 7084 (1991)
- [15] B.J. Archer, G.A. Parker and R.T. Pack, Phys. Rev. A41, 1303 (1990)
- [16] C.D. Lin, Adv. Atom. Mol. Phys. 22, 77 (1986)
- [17] V.V. Gusev et al, Few-Body Systems 9, 137 (1990)
- [18] M. Decker, W. Sandhas and V.B. Belyaev, Phys. Rev. A53, 726 (1996)
- [19] S. Hara and T. Ishihara, Phys. Rev. A39, 5633 (1989)
- [20] W. Czaplinski et al., Z. Phys. D37, 283 (1996)

Received by Publishing Department
on November 19, 1996.

Беляев В.Б. и др.

E4-96-429

Скорости распада и спектры излучения HeH μ

Исследован радиационный и безызлучательный распад зарядово-несимметричных молекулярных ионов $^{3,4}\text{He}^{1,2}\text{H}\mu$. Метод поверхностных гиперсферических функций использован для расчета вероятностей распада и спектров γ -излучения для состояний с полным угловым моментом $L=0,1,2$. Рассмотрена изотопическая зависимость скоростей распада. Сравнение рассчитанных спектров γ -излучения с последними экспериментальными данными подтверждает предположение о распаде HeH μ из состояний с $L=1$.

Работа выполнена в Лаборатории теоретической физики им. Н.Н.Боголюбова и Лаборатории вычислительной техники и автоматизации ОИЯИ.

Препринт Объединенного института ядерных исследований. Дубна, 1996

Belyaev V.B. et al.

E4-96-429

Decay Rates and γ -Ray Spectra of HeH μ Systems

Radiative and nonradiative decays of charge non-symmetrical molecular ions $^{3,4}\text{He}^{1,2}\text{H}\mu$ have been investigated. Decay rates in both channels and γ -ray spectra for the states of the total angular momentum $L=0,1,2$ have been calculated using the hyperspherical «surface» function method. Isotopic dependence of the decay rates is discussed. A comparison of the calculated γ -ray spectra with recent experiments confirms the assumption of the HeH μ decay from the $L=1$ state.

The investigation has been performed at the Bogoliubov Laboratory of Theoretical Physics and Laboratory of Computing Techniques and Automation, JINR.

Preprint of the Joint Institute for Nuclear Research. Dubna, 1996